

Acoustic response of phospholipid membranes: Estimating thermodynamic susceptibilities from fluorescence spectrum

Shamit Shrivastava¹, Matthias F. Schneider², Robin O. Cleveland¹

1. Institute for Biomedical Engineering, University of Oxford, Oxford OX3 7DQ, UK

2. Medizinische und Biologische Physik, Technische Universität Dortmund, Otto-Hahn Str. 4, 44227 Dortmund, Germany

Membrane-protein systems constitute an important avenue for a variety of targeted therapies. The ability to alter these systems remotely via physical fields is highly desirable for the advance of noninvasive therapies. Biophysical action of acoustic fields in particular holds immense potential for applications in drug delivery and neuro-modulation. Here we investigate the optical response of solvato-chromic fluorescent probe Laurdan, embedded in multilamellar lipid vesicles, subjected to broadband pressure impulses of the order of 1Mpa peak amplitude and pulse width of less than 10 μ s. The response is quantified in terms of the shift in fluorescence spectra using a ratiometric technique. Based on the fluctuation dissipation theorem applied to a coupled membrane-fluorophore system, it is shown that the perturbation of the fluorescence spectra of embedded molecules to the pressure impulses is determined by the thermodynamic state of the interface, or in other words, the thermodynamic susceptibilities such as the compressibility or heat capacity of the system. However, given that the thermodynamic susceptibilities of such systems, especially in native biological environment, are not easy to obtain experimentally, a necessary corollary to the thermodynamic approach is derived. This establishes a direct relation between the width of the emission spectra and the thermodynamic susceptibilities of the system. The result has practical importance as it gives access to the thermodynamic properties of the membrane from steady state fluorescence measurement without the need to perturb the system. Simply stated, the experiments show that the magnitude of the perturbation response of a membrane system to an acoustic insult is proportional to the width of the emission spectrum of the embedded membrane probe. Finally, there exists a direct correlation between the solvation (miscibility) and permeation of a molecule through a membrane and the implications of this study for acoustically induced enhanced permeability of the membrane are discussed.

Introduction

Biophysical mechanisms that underline the interaction of acoustic radiation with biological material, especially cellular membranes are of interest because of their possible application in noninvasive ultrasound and shockwave therapies. Behavior of functional molecules embedded in a membrane environment when exposed to an acoustic field is of interest for understanding, for e.g. acoustically triggered membrane permeabilization (“sonoporation”) and neuromodulation (Legon et al., 2014). Physical mechanisms underlying the acoustic properties of biological materials have been investigated previously. Floyd Dunn pioneered the research into these mechanisms by establishing phenomenological relationships between the thermodynamic state variables (pressure, pH, temperature) of biological macromolecules and their acoustic properties (absorption and sound velocity) in aqueous suspensions (Kessler and Dunn, 1969; O’Brien and Dunn, 1972). Artificial lipid membranes in the form of multi-lamellar lipid vesicles were also investigated and an analytical relationship was established between the compressibility of the membrane interface and absorption and velocity of sound through the vesicle suspension (Tatavol and Dunn, 1992). The role of increased acoustic in the membrane and its relation to enhanced permeability was also underlined. However lately, model based approaches, somewhat disconnected from the earlier analytical works in the field, have been guiding the research where the emphasis has been on understanding the aforementioned biophysical mechanisms in terms of presumed motion of microscopic structures in space and time (Koshiyama et al., 2006; Krasovitski et al., 2011). These recent work have taken a more literal approach to “sonoporation” where the formation of physical pores in the membrane is assumed a priori as a mechanism for acoustically induced enhanced permeability of the membrane (Kudo et al., 2009; Zhou et al., 2009). It is important to recall that a membrane is not a simple physical barrier that has to be perforated in order to be permeable but it can reorganize around the permeant at an entropic cost via reversible fluctuations (Wunderlich et al., 2009). Indeed, the permeability of molecules can be described as a linear function of the partition coefficient (miscibility) of the permeant in the membrane while the slope is determined by the molecular size (Diamond and Katz, 1974). Therefore the solvation state or the hydration state of the permeant-membrane complex that exists as an intermediate during permeation is critical for rate determination (Marcus and Amos, 1985). Understanding how the solvation state can be modified acoustically is therefore necessary for understanding the phenomenon of “sonoporation”. While formation of physical pores during enhanced permeability

is certainly one of the possibilities, an approach that assumes such a mechanism a priori would also require a priori assumption about the nature of water in these pores, which is not trivial (Xin Chen et al., 2007; Zheng et al., 2006; Zhu and Granick, 2001). Such assumptions also discount the possibility of any synergistic role of the conformational changes in the permeant-membrane complex during the process (Seeger et al., 2010). A complete molecular-mechanical theory although highly desirable is impractical especially given the enormous degrees of freedom presented by biological systems. As a result, the link between physical effects and the chemical or biological activity is not addressed comprehensively by such models. Here we take a fundamental approach (Einstein, 1919) starting from the experimental observations and second law of thermodynamics to establish an analytical relationship describing perturbation in the energy states of a membrane bound fluorescent probe as a result of a pressure impulse.

Fluorescent molecules known as “solvato-chromic” dyes such as Laurdan, Prodan, di-4-anepdhq etc (Bondar and Rowe, 1999; Kusube et al., 2005; Lorizate et al., 2009; Lúcio et al., 2010; Owen and Gaus, 2009; Owen et al., 2006; Parasassi et al., 1990, 1998; Sanchez et al., 2012; Szilágyi et al., 2008; Sýkora et al., 2009; De Vequi-Suplicy et al., 2006; Viard et al., 1997, 2001; Wang et al., 2009) as well as “electro-chromic” (voltage sensitive) dyes such as di-8-anneps and RH421 (Clarke and Kane, 1997) are known to have spectral properties that are sensitive to their dielectric environment. These molecules are designed to exhibit a high ground state and/or transition dipole moments compared to otherwise “non-sensitive” probes and as a result do significantly more work in a dielectric environment. This results in an environment sensitive shift in the absorption and emission spectrum of these dyes. In this study we employ Laurdan, which has been used extensively in membrane studies (Table 1). The emission spectrum of the dye shows a red shift as the membrane becomes more hydrated or fluid like. In particular, it shows a large (40-60nm) and abrupt shift in the peak emission wavelength when the membrane goes through gel-fluid phase transition. Since the spectrum behaves as a function of the state of the system, it undergoes an abrupt change, invariant of whether the state changes as a function of temperature (Parasassi et al., 1991) or pressure (Kusube et al., 2005). Therefore, theoretically it should be possible to see such changes dynamically as well during a pressure impulse. Experimentally, a change in position or shape of the spectrum can also be quantified by the ratio of intensities at two different fixed wavelengths. The resulting value, to be referred as Ratio-metric Parameter (RP), and its variant,

Generalized Polarization ($GP=(RP-1)/(RP+1)$) which is more common in literature as it behaves similar to a general order-parameter for a system undergoing phase transition (Harris, 2002).

The aim here is to establish a state invariant interrelationship between various measurable thermodynamic properties of the system that includes the specific heat and compressibility of the membrane, emission spectrum of Laurdan, the applied pressure impulse and the resulting synchronous changes in the RP.

Materials and Methods

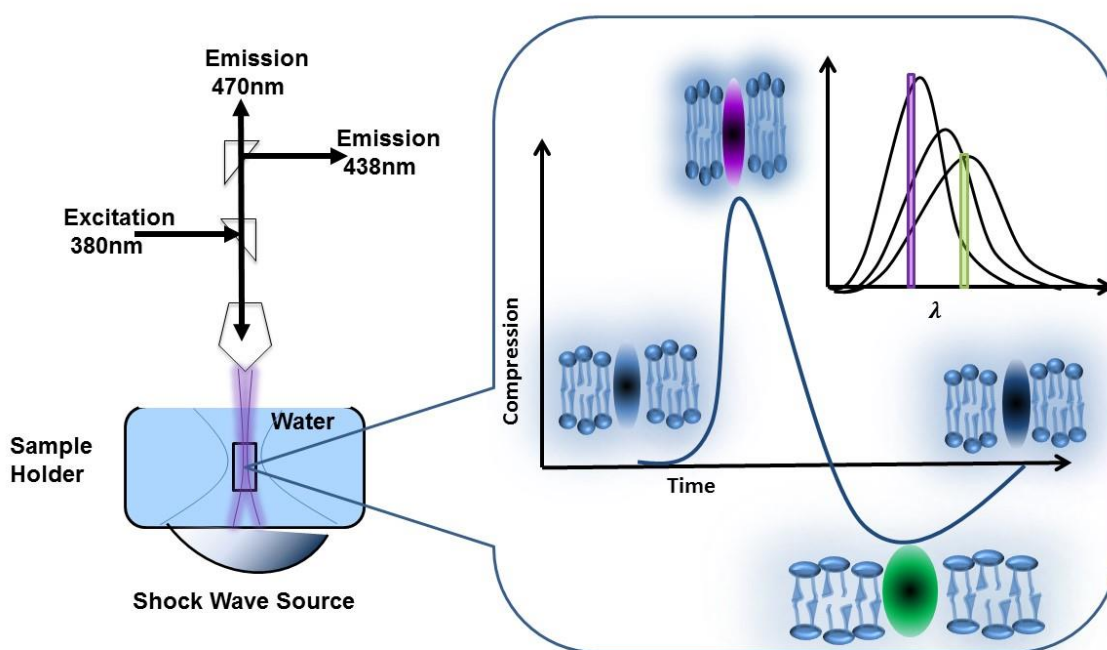


Figure 1 Experimental Setup A shock wave source coupled to a water tank provides the pressure impulse at its focus which coincides with the focus of the optical setup. The temperature controlled water tank has multilamellar lipid vesicles (MLVs), embedded with the dye Laurdan, present everywhere. As the pressure impulse interacts with the lipid vesicles, the emission spectrum shifts in opposite directions based on condensation or expansions, as indicated in the schematic on the right. The shift is quantified ratiometrically by the two photomultiplier tubes recording simultaneously at two different wavelengths (438 and 470nm).

Materials:

The lipids 1,2-dioleoyl-sn-glycero-3-phosphocholine (DOPC 850375), 1,2-dimyristoyl-sn-glycero-3-phosphocholine (DMPC 850345), 1,2-dipalmitoyl-sn-glycero-3-phosphocholine (DPPC 850355) were purchased as a 25 mg/mL solution in chloroform from Avanti Polar Lipids, Inc., Alabaster, AL, USA. Laurdan was purchased from Life technologies, USA. Unless otherwise stated, all other chemicals were purchased from Sigma Aldrich.

Preparation of multilamellar vesicles (MLVs):

100 ul of the lipids (DOPC, DMPC or DPPC) (25mg/ml), from the chloroform stock without any further purification, were dried in a 10 ml glass vial overnight in a vacuum desiccator. The dried film was rehydrate in 5 ml MilliQ ultrapure water and heated for 30 mins on a hot plate at 50°C with the cap tightly sealed. The film was then vortexed at 2000 rpm for 30 seconds and the processes repeated once more to get the MLVs suspension. 1ul of a 50mg/ml solution of Laurdan in DMSO (dimethyl sulfoxide) was added to 5ml of MLV suspension, which was then mixed with 500ml of additional MilliQ water in the temperature regulated tank.

Optical and pressure measurements and data analysis:

A custom optical setup was built for dynamic ratiometric measurements. A high power light emitting diode (Thorlabs) was used as the excitation source with a central wavelength of 385nm followed by a bandpass filter (390 \pm 20nm). A dichoric mirror (414 nm) then separated the excited and emitted light, with the reflected light focused at the back focal plane of LWD M PLAN FL 20X Objective (Olympus) with a working distance of 13mm. The emitted fluorescence was split by another dichoric at 452 nm collected by two Hamamatsu photomultiplier tube (H10493-003) across two bandpass filters at 438 (\pm 12nm) and 470 nm (\pm 11nm). The pressure waveform was measured using a needle hydrophone from Muller Instruments with a sensitivity of 12.5mV/Mpa (bandwidth 0.3 – 11 MHz \pm 3.0 dB). It was used to locate the focus and measure the pressure waveform at the focus of the shockwave source (Swiss Piezoclast).

Data was acquired using NI PCI 5122 dual channel simultaneous 100Ms/s digitizer and was analyzed using NI Labview. LED was triggered 5 ms before the shock for a duration 10 ms around each shock. Shocks were fired at 3Hz repetition rate and data was acquired for 500 μ s of which 50

μs preceded the trigger. Each waveform was sampled down by 10 points average making the effective sampling rate as 10MS/s and bandwidth of 5MHz, which is less than the 8Mhz bandwidth of the PMTs. First 10us were taken as the base signal corresponding to the mean state of the system, I_0 for each channel. The overall waveform from each channel was normalized with respect to the corresponding base values to obtain relative intensity changes ($\frac{\Delta I}{I_0} = \frac{I}{I_0} - 1$). The ratiometric difference ($\Delta RP/_{RP}$) obtained from the individual intensity changes as in $\Delta RP/_{RP} = \left(\frac{\Delta I}{I_0}\right)_{438nm} - \left(\frac{\Delta I}{I_0}\right)_{470nm}$, where $RP = I_{438nm}/I_{470nm}$. This minimizes extraneous signals, such as concentration inhomogeneities, background fluorescence and purely mechanical undulations in the field of view (motion of any surfaces in the experimental setup) that are otherwise inconsequential for the state of the lipid interface (Shrivastava and Schneider, 2014)

Results

Aqueous suspension of MLVs of different lipids and different states were exposed to pressure impulses and ratiometric response was obtained using the optical setup described in figure 1. The results have been summarized in figure 2. DPPC with the main fluid-gel phase transition temperature as $T_{pt} = 41^\circ\text{C}$ (Parasassi et al., 1991) is in the most ordered state at 20°C among the samples being tested. This is indicated by the reduced temperature defined as $T^* = \frac{T - T_{pt}}{T_{pt}} = -0.067$ when temperatures are in Kelvin. Similarly DMPC (Needham and Evans, 1988) with $T_{pt} = 23.4^\circ\text{C}$ set at 10°C , 23°C and 37°C represent successively more disordered states. DOPC with $T_{pt} = -20^\circ\text{C}$ (A~ta et al., 1994) represents the most disordered state at 20°C . As can be seen in figure 2, reduced temperature allows us to represent different lipid formulations on the same temperature axis which shows direct correlation with the observed RP, underlining the significance of RP as an order parameter for the main gel-fluid transition in lipid systems. Indeed, given that significant temperature gradient were present in the water tank, the mean RP value is more reliable parameter here that defines the mean state.

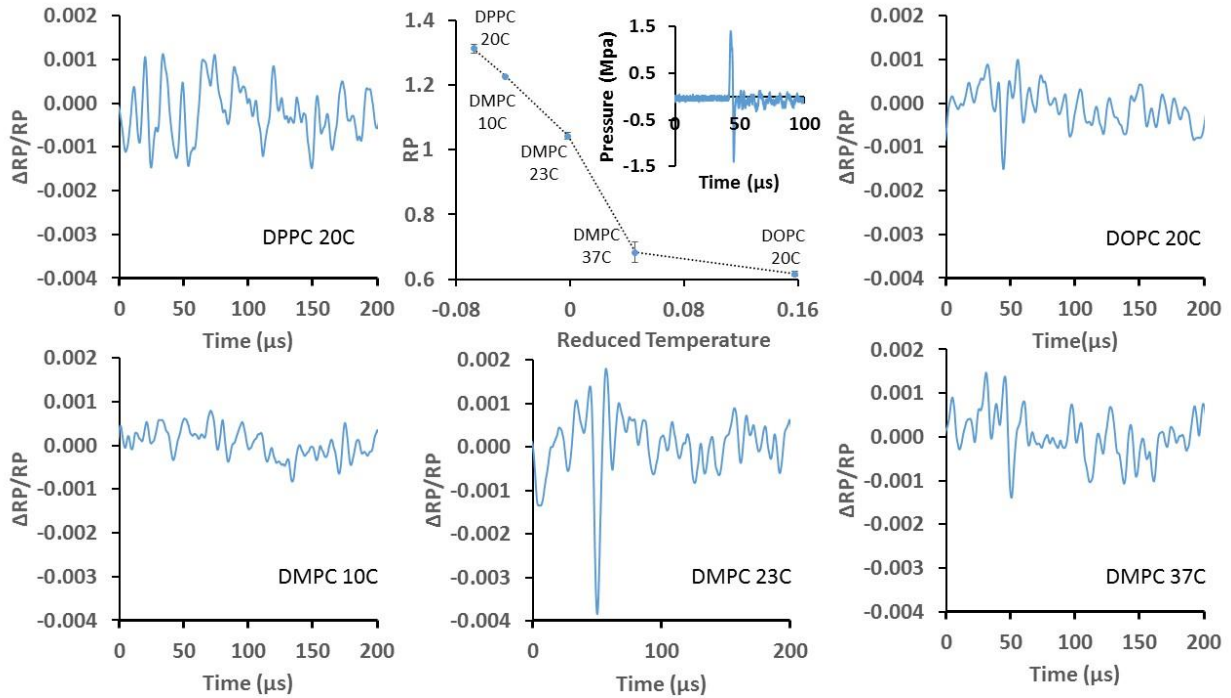


Figure 2 Perturbation response as a function of state (Top Center) Shows the mean or equilibrium RP value calculated from Laurdan emission in different MLV formulations, plotted as a function of the respective reduced temperatures. The inset shows the waveform for the pressure impulse applied to these systems (peak pressures $\pm 1.81\text{Mpa}$). The average responses ($n=500$, Low-Pass 100kHz) are quantified by the change $\Delta RP/RP$ plotted as a function of time for the different MLV systems, indicated by the respective legend on each plot.

The perturbation $\Delta RP/RP$, when these samples were subjected to pressure impulse (peak pressure $\pm 1.81\text{Mpa}$) is plotted as a function of time (fig.2). The impulse is fired at $t = 0\mu\text{s}$ and can be seen to arrive around $t = 50\mu\text{s}$ whenever the signal is significant. Interestingly, only a negative response is observed when it is significant, with the maximum response of $\Delta RP/RP \sim 0.004$ obtained from DMPC at 23°C , i.e the system that is closest to phase transition ($T^* \approx 0$). In the gel phase, the observed $\Delta RP/RP < 0.001$ (the noise level) in both the systems that were in gel state ($T^* < 0$), i.e. DPPC at 20°C and DMPC at 10°C . The intermediate response of $\Delta RP/RP \sim 0.0015$ is observed for both DMPC at 37°C and DOPC at 20°C that were in fluid state ($T^* > 0$). Clearly the response $\Delta RP/RP$ of the membrane is a function of state (here order parameter RP and temperature) and is not monotonic.

To see if the values of $\Delta RP/RP$ make sense quantitatively, we look at $\Delta RP/RP \sim 0.004$ in the transition region. Given that RP behaves similar to an order parameter, in the transition region one can make the approximation $\Delta RP/RP \sim \Delta V/V$ (Shrivastava and Schneider, 2013), which will be discussed in greater detail below. Typical volume increase associated with lipid phase transitions in DMPC under quasistatic conditions is known to be of the order of $\frac{\Delta V}{V} \sim 3\%$ (Halstenberg et al., 1998; Krivanek et al., 2008). Given that in same region the $\Delta RP/RP$ changes by -0.44 , gives an average coupling coefficient in the transition region. Thermodynamically, the amplitude response in volume $\frac{\Delta V}{V}$ can be related to pressure amplitude in linear approximation as $k_s = -\frac{\Delta V}{V} \frac{1}{\Delta P}$, where k_s is the adiabatic compressibility of the system. From measurements reported elsewhere, k_s would typically range from 3.1×10^{-11} to $5.27 \times 10^{-11} \text{ cm}^2/\text{dyne}$, going from gel state to liquid state in DMPC MLVs (Krivanek et al., 2008). Therefore the expected range for $\Delta RP/RP$, in region where $\Delta RP/RP = \text{const.} \Delta V/V$ is valid, would be from -0.004 to -0.007 . This fits the observation rather well given the first order nature of the calculation. Indeed, calculations based on adiabatic compressibility that were measured using low intensity ultrasound ($\sim 10^{-6} \text{ W/cm}^2$) are expected to overestimate the large amplitude response. For example, for a change in peak negative pressure from -1.63 Mpa to -1.81 Mpa , the peak negative $\Delta RP/RP$ was observed to change from 1.11×10^{-3} to 1.15×10^{-3} . But for a further increase in peak negative from -1.81 MPa to -1.99 MPa , $\Delta RP/RP$ does not increase significantly anymore with a value of 1.155×10^{-3} indicating nonlinear saturation in response.

Coming to the sign of perturbation, it is important to consider the relaxation times in lipid membranes. Experimentally distinct time scales have previously been identified by others in several different lipid systems when lipid vesicles were exposed to photo-thermal shocks (1°C temperature rise in 1ns) (Holzwarth, 1989). Broadly these time scales can be associated with formation of a kink in the lipid tail (1-10ns), rotation of lipids (100ns), lateral diffusion (1-10 μs), formation of domains (100 μs) and phase separation ($>1\text{ms}$). In comparison to the front, the pressure negative tail of the impulse consists of longer time scales which are comparable to the lateral diffusion (1-10 μs) range of the relaxation times in lipids. Changes in the lipid tail conformation (1-10ns) or rotation of lipids (100ns) that could happen in the pressure positive phase

of the impulse would only alter the environment of the probe at lateral diffusion (1-10 μ s) timescale and hence a positive $\Delta RP/RP$ might not be observed at these timescales (Holzwarth, 1089). There is also the possibility of action of the impulse through water-to-vapor transition *near* the interface, which can take place in the expansion phase of the pulse. Indeed, at higher pressure amplitudes we observed clear signs of cavitation at the interface which will be discussed elsewhere. The discussion here is limited to the finite amplitude pressure impulse where the membrane responds in accordance with the fluctuation dissipation theorem, allowing quantitative predictions at infinitesimal amplitudes and correct orders of magnitude for finite amplitude pressure impulses, as discussed below.

Mechanisms

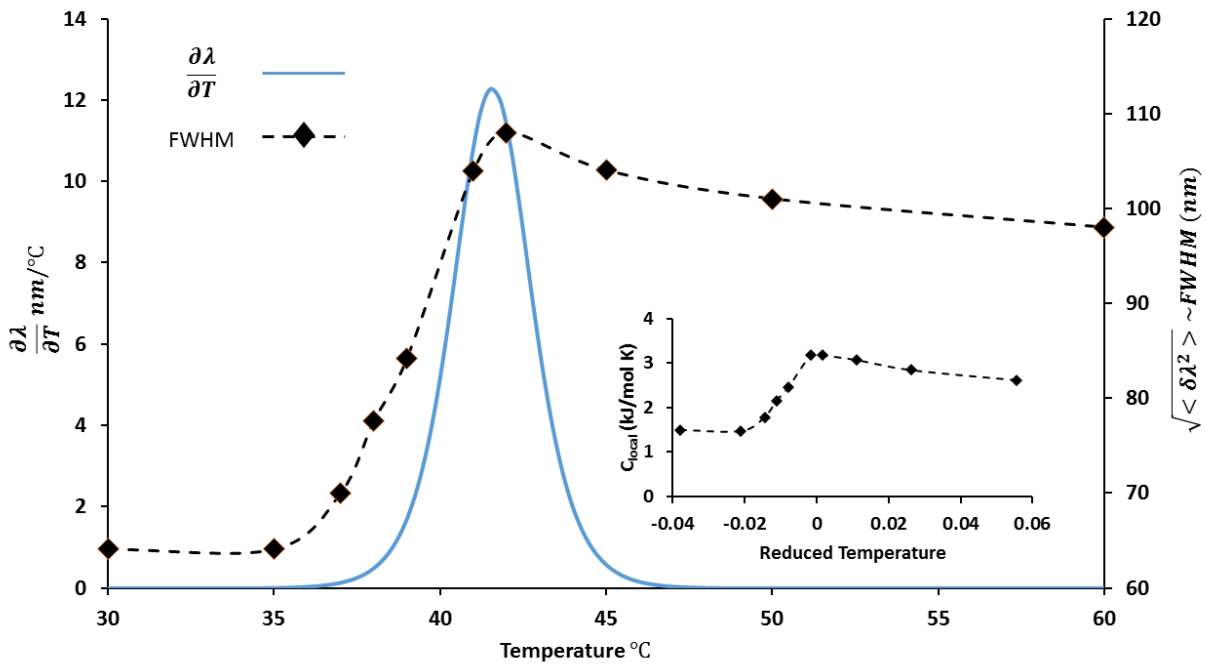


Figure 3 Estimating specific heat from observed emission spectrum of Laurdan *The rate of change of peak emission wavelength with respect to temperature $\frac{\partial \lambda}{\partial T}$ as obtained from reported emission spectrums in (Parasassi et al., 1991) is plotted as a function of temperature. From the same emission spectrum, FWHM were obtained and have been plotted on secondary axis. The inset shows the specific heat calculated from these optical measurements and using a constant fit parameter of proportionality.*

These experiments on artificial membrane systems, predesigned for a desired thermodynamic state in a controlled environment, have helped us appreciate the non-monotonic relationship between the state and how the energy spectrum of molecules embedded in these systems is perturbed by a pressure impulse. As discussed, the nature of these perturbations is consistent in phenomenological sense. However, a more fundamental microscopic understanding of how changes in membrane manifest as changes in the fluorescence spectrum of the an embedded fluorophore are desirable. From a theoretical point of view, the rationale of using macroscopic measurements on artificial membranes is to establish the microscopic nature of the general principles that can then be applied in more complex systems *locally*. This has immense practical application especially from a biological point of view, where unlike artificial single component lipid membrane, significant local heterogeneities are present. Furthermore, material properties such as compressibility and specific heat present in the equations of phenomenological model are hard to measure in native biological systems and are almost impossible to measure locally. A microscopic understanding of the process that allows predictions based purely on optical measurements would be highly desirable. Also as discussed, understanding acoustically induced changes in interfacial solvent environment has direct implications for controlled permeation of cellular membranes.

The fluorescence phenomenon, even though represented by a single molecule in its local environment, is an ensemble property of the system. The energy of a photon that is absorbed or emitted represents the energy difference between the ground and excited states of the corresponding fluorophore that belongs to the ensemble. Hence the width of the spectrum of a fluorescence molecule depends strongly on the statistical distribution of states accessible to an ensemble during absorption or emission, which in turn should increase with an increase in conformational space. When the dye belongs to a hydrated interface such as a lipid membrane, this conformational space also includes various arrangements with lipid and water molecules that are allowed for the given macroscopic state of the entire system. For example, a shift in emission or absorption maximum $h\Delta\nu$ of electro or solvato-chromatic dye is mainly attributed to the work done by the transition dipole (emission) or ground state dipole (absorption) respectively, on the solvent environment, which is significant for charge-transfer probes due to stronger dipole interactions making them, for instance, “voltage sensitive”(Bublitz and Boxer, 1997). As a first order approximation $h\Delta\nu_{shift} = \Delta E_{solv} \sim \mathbf{F}_0 \cdot \Delta \mathbf{M}_{solv}$ is the electrical work done on the solvent in the frame of reference of the dye to reach the relaxed state, also known as solvent relaxation. Here \mathbf{F}_0

is average electric field of the ground state dipole (absorption) or of the transition dipole (emission) of the dye and $\Delta\mathbf{M}_{solv}$ is the change in average solvent dipole during solvation. Furthermore then $\langle \Delta E_{solv}^2 \rangle \sim \langle \Delta\mathbf{M}_{solv}^2 \rangle \sim T^2\epsilon$, where ϵ is the dielectric constant of the interface analogous to solvent relaxation in bulk along the lines of Marcus and Fraunfelder (Fenimore et al., 2004; Frauenfelder et al., 2009; Marcus and Amos, 1985; Prakash and Marcus, 2007). Similarly, one should expect a pressure (\mathbf{P}) dependent change in the spectrum of a photoactive molecule $h\Delta\nu_{shift} = \Delta E_{solv} \sim \mathbf{P} \cdot \Delta\mathbf{V}_{solv}$ if it undergoes significant structural change and hence a volume change ($\Delta\mathbf{V}_{solv}$) on irradiation (Frauenfelder et al., 1990; Mauring et al., 2005). Indeed, molecules that can undergo photo isomerization (for eg. Azobenzene and its derivatives) show significant spectral shift as a function of pressure (Effects, 1984; Kadhim, 1966; Shimomura and Kunitake, 1987) and provide us with an avenue to develop “mechano-sensitive” dyes.

For a more general description, let E_1 be the (internal) energy of the dye (subsystem 1) which is in equilibrium with the interface. Then let E_2 be the energy of the rest of the interface (subsystem 2). The number of ways the total energy can be distributed in these two compartments given that the two systems interact and the individual probabilities are not independent ($W(E_1, E_2) \neq W(E_1) \cdot W(E_2)$) is a function of the entropy of the entire system (Chowdhury and Chanda, 2012). Taking a heuristic point of view and noting that an interface has its own specific heat and entropy decoupled from the bulk (Einstein, 1901), the entropy of the interfacial system is defined as $S(E_1, E_2)$ (Einstein, 1911) which gives the probability distribution function as;

$$dW = const. e^{S(E_1, E_2)} dE_1 dE_2 \quad (1)$$

Realizing that the most probable energy state E_1^0 of the dye lies at the maximum of entropy potential, the Taylor expansion of the entropy up to second term near (E_1^0, E_2^0) can be written as;

$$S(E_1, E_2)_{E_1^0, E_2^0} = \frac{\partial S}{\partial E_1} \delta E_1 + \frac{\partial S}{\partial E_2} \delta E_2 + \frac{1}{2} \frac{\partial^2 S}{\partial E_1^2} (\delta E_1)^2 + \frac{1}{2} \frac{\partial^2 S}{\partial E_2^2} (\delta E_2)^2 + \frac{\partial^2 S}{\partial E_1 \partial E_2} \delta E_1 \delta E_2 \quad (2)$$

As there is an entropy maximum at (E_1^0, E_2^0) , we have $\frac{\partial S}{\partial E_1} = \frac{\partial S}{\partial E_2} = 0$ while $\delta E_1 = E_1 - E_1^0$ and so on. Furthermore, using the definition of heat capacity $C = \frac{\partial E}{\partial T}$ eq.(2) can be reduced to (Einstein, 1910);

$$S(E_1, E_2)_{E_1^0, E_2^0} = -\frac{1}{2} \left\{ \frac{(\delta E_1)^2}{C_1 T_1^2} + \frac{(\delta E_2)^2}{C_2 T_2^2} + \frac{\delta E_1 \delta E_2}{T_2^2} \frac{\partial T_2}{\partial E_1} \right\} \quad (3)$$

Therefore, the energy fluctuations in the two systems are not only governed by the heat capacities of the respective systems

$$\langle (\delta E_i)^2 \rangle \sim C_i T_i^2 \quad (i = 1 \text{ or } 2), \quad (4a)$$

but are also coupled

$$\langle \delta E_1 \delta E_2 \rangle \sim T_2^2 \left(\frac{\partial T_2}{\partial E_1} \right)^{-1} \quad (4b)$$

Here T includes Boltzmann constant k and hence has the units of energy. Going back to the fluorophore membrane system, E_1 is the (internal) energy of the dye (subsystem 1) and is directly related to the mean radiation energy E_r absorbed or emitted by the fluorophore as per the first law;

$$E_1^* - E_1 = E_r(\lambda) \quad (5)$$

Here E_1^* is the energy of the electronic state immediately upon absorption or emission which is essentially instantaneous ($\sim 10^{-15}$ sec) (Jaffe and Miller, 1966) and can be assumed to be independent of any rearrangement in hydration shell ($\sim 10^{-12}$ sec) where λ is the wavelength of radiation. Therefore any variation in $E_r(\lambda)$ due to rearrangement of the hydration shell can be attributed mainly to variations in E_1 , i.e. only the relaxed state energy distribution of the dye molecules¹. From Maxwell theory, the spectrum ρ_λ (radiation density) and the corresponding mean radiation energy absorbed or emitted $E_r(\lambda)$ are related as (Einstein, 1909)

$$E_r(\lambda) = \frac{L^3 \lambda^2}{8\pi c^2} \rho_\lambda \quad (6a)$$

¹ Since we are interested in fluctuations in E_1 , E_1^* is assumed constant for the simplicity of analytical results. In general an increase in the distribution of the radiation would result from addition of the increase in distributions of both the ground and the excited states of the dye molecules $\delta E_1^{*2} + \delta E_1^2 = \delta E_r^2$, (properly $S(E_1, E_1^*, E_2)$ written for steady state) as a result of change in the state of the hydration layer. Thus an increase in distribution of radiation still reports an increase in fluctuations of the hydration layer and the assumption regarding E_1^* , although justified by the timescales, is not necessary.

If λ_{max} is the observable that determines the state phenomenologically based on Einstein's description of entropy potential, then using $\left(\frac{d\rho\lambda}{d\lambda}\right)_{\lambda_{max}} = 0$ and for a normalized distribution ($\rho_{\lambda_{max}} = 1$),

$$\left(\frac{dE_r}{dT}\right)_{\lambda_{max}} = \frac{L^3\lambda_{max}}{4\pi c^2} \frac{d\lambda_{max}}{dT} \quad (6b)$$

Then from eq. (5) and (6b) we have $\langle \delta E_1^2 \rangle \sim \langle \delta \lambda_{max}^2 \rangle$. Now either by propagating the error in $E_r(\lambda)$ to λ , or by redefining the entropy potential phenomenologically as $S(\lambda_{max}, E_2)$ (Kaufmann, 1989) and using eq.(4), (5), (6) following relation can be derived after dropping the constants

$$\langle \delta \lambda_{max} \delta E_2 \rangle \sim -T^2 \lambda_{max} \left(\frac{\partial T}{\partial \lambda_{max}}\right)^{-1} \quad (7)$$

Here $\delta \lambda_{max}$ is the fluctuation or perturbation in the wavelength of radiation absorbed or emitted by the ensemble of dye molecules (subsystem 1), which is coupled to the fluctuations or perturbation δE_2 of the membrane (for instance due to a pressure impulse) via the state dependent coupling parameter $\left(\frac{\partial T}{\partial \lambda_{max}}\right)^{-1}$ which is experimentally accessible and is essentially the change in mean or peak absorption or emission wavelength. The term is plotted as function of temperature in fig. 3 for DPPC MLVs and shows strong correlation with the specific heat (Grabitz et al., 2002) allowing us to write

$$\left(\frac{\partial T}{\partial \lambda}\right)^{-1} \sim C \text{ or using eq. 7, } \Delta \lambda_{max} \sim \Delta E_2 \quad (8)$$

where C is the heat capacity of the system. Thus the λ_{max} is directly correlated to the energy of the surrounding membrane and the strength of coupling is determined phenomenologically by the constants of proportionality in eq.(8). Conditions when such an assumption is valid, in general, have been discussed previously in detail by others for fluctuation correlations in lipid systems (Heimburg, 1998; Shrivastava and Schneider, 2013; Steppich et al., 2010). In fact, together with these earlier works the following has now been observed;

$$\frac{\Delta \lambda}{\lambda} \sim \frac{\Delta E}{E} \sim \frac{\Delta V}{V} \sim \frac{\Delta A}{A} \sim \frac{\Delta I}{I} \sim \frac{\Delta \mu}{\mu} \quad (9)$$

In addition to already introduced variables, I is the absolute intensity at fixed wavelength or polarization or the intensity. In fact I can represent the optical observable even for non-fluorescence measurements such as transmission, which is again closely related to μ (Shrivastava and Schneider, 2013), the average dipole moment at the interface. Note that strong coupling between the embedded molecule and the membrane has a significant impact not only on the embedded molecule but also on the membrane, which can alter the properties of the environment locally as well as globally (Papahadjopoulos and Moscarello, 1975). So in that respect λ is different from other observables. However, extending this relation to λ gives direct access to the nature of local energy landscape in the form of $\langle \delta\lambda^2 \rangle$ through simple instrumentation and allows us to appreciate how the macroscopic state of the system can dominate this landscape, which was not possible before. In fact, using eq (7) and (8) one can write;

$$\frac{\Delta\Gamma}{\lambda_{max}} \sim T \cdot C(T) \quad (10)$$

Where $\Delta\Gamma = \sqrt{\Gamma^2 - \Gamma_0^2}$ can be approximated by *excess* FWHM from spectrums of Laurdan plotted for DPPC in Fig.3 as reported by others (Parasassi et al., 1991). Then C_{local} as observed from Laurdan is plotted in the inset (fig .3) using a phenomenological constant of proportionality $\varepsilon = 5000 kJ.mol^{-1}$ and $\Gamma_0 \approx 50nm$ approximated as FWHM of Laurdan in n-hexane (Titova et al., 2014). The obtained C_{local} predicts the macroscopic excess C_p rather accurately (Heimburg, 1998; Wunderlich et al., 2009) when the state changes from gel to the transition region, however it doesn't decrease as significantly as macroscopically measured C_p when moving from gel to fluid state. This behavior is remarkably similar to quantum statistical C_p calculated by Wilkinson and Nagle based on a hindered harmonic potential (Wilkinson and Nagle, 1982) and might provide further insights into the observed microscopic nature of specific heat in lipid environment. For example, the effects of increased hydration on the energy distribution of embedded molecules due to formation of hydrogen bonds (Poperscu et al., 2013). Note that we have made no assumption regarding the nature of interaction between the fluorophore and membrane, for e.g. whether its "electro-chromic" or "solvato-chromic". Still, while thermodynamics can explain the implications of a given value $\left(\frac{\partial T}{\partial \lambda}\right)^{-1}$ for the coupling term $\langle \delta\lambda\delta E \rangle$ but not why they couple, at least not without further knowledge on the structure of the molecules and *mechanistic* assumptions

(placement and orientation vs hydration, charge interaction) about the nature of interaction between the fluorophore and its local environment. While the fluorescence phenomenon is local, it's the imposition of entropy law for the entire system (eq.2) that makes the fluorescence behaves as an integrated variable of the state.

The relationships derived here attribute a thermodynamic meaning to the fluorescence spectra that significantly differs from how fluorescence data is currently interpreted in such systems (Parasassi et al., 1990). Usually fluorescence spectra is interpreted in structural terms of “tight” packing of the molecule into the bilayer and the resulting water content of its surroundings (Bagatolli, 2003; Harris et al., 2002; Parasassi et al., 1991). In model pure lipid vesicles, which show clear phase separation, the broadening during the transition can be partially attributed to the coexistence of the phase separated domains as given by the lever rule applied to a first order phase transition (Parasassi et al., 1990, 1993; Sanchez et al., 2012). However, multi-component system on the other hand can approach a critical limit where most of the molecules exist at a domain boundary (Honerkamp-Smith et al., 2008) and in these systems the spectral fluctuation are expected to become evident at single molecule level (Wazawa et al., 2000) and can be investigated using, for instance, Fluorescence correlation spectroscopy (FCS)(Rigler, 2010). Interestingly in many biological systems, in the absence of direct evidence of phase separated domain like structures, fluorescence spectra show significant shift and state dependent broadening (Hazel et al., 1998; Lorizate et al., 2009; Sýkora et al., 2009; Toyoda et al., 2009; Vanounou et al., 2002). In these cases while the structural interpretation remains ambiguous, researchers are debating transient phase separated microdomains, known as lipid rafts (Munro, 2003; Sanchez et al., 2012), similar to fluctuating micro or nano domains that exist near a criticality (Honerkamp-Smith et al., 2008) but are difficult to resolve experimentally. Eq. (1), (3) and (10) on the other hand provide a thermodynamic meaning of the spectral width in terms of the heat capacity C of the environment that does not require such a structural interpretation.

The principle that has been shown to be at work when state and hence the spectrum of Laurdan changes as a result of pressure or temperature also explains the change in spectrum of Laurdan due to the introduction of other nonspecific molecules in the system, such as cholesterol, detergents, drugs, alcohol and other ingredients (Table 1). State changes due to various molecular agents have been measured using Laurdan, they have been tabulated in Table 1 along with the corresponding

references. Given that the presented theory unifies a wide extent of observations made with Laurdan in artificial systems, it remains to be seen how far these principles can be applied to dynamic process in Biology with all its heterogeneity intact. Experiments done previously by Tasaki on Nerve fibers during an action-potential present a promising outlook, where the width of the emission spectrum was observed to shrink at the peak amplitude (Tasaki et al., 1973). Independently Luzzatti et.al, showed independently using X-ray diffraction measurements that the nerve gets stiffer at the peak amplitude (Luzzati et al., 1999), as the work presented here would have predicted.

Finally coming back to “sonoporation”, since the emission spectrum of the fluorophore is directly related to its solvation state at the interface, acoustically induced shift in the emission spectrum indicates, in general, a change in the solvation of a permeant in the membrane. A negative value for $\Delta RP/ RP$ represents an increase in hydration of the dye molecule, which to a first order can be assumed to be similar for similar molecules penetrating the membrane (Engelk et al., 2001). Hence a negative $\Delta RP/ RP$ is equivalent to a decrease in activation barrier for hydrophilic molecules and its relative drop can be seen to be maximum near a transition or peak in the compressibility or the heat capacity of the membrane (Fig.2). While this result at first might appear to be rather specific to a particular lipid composition at a particular temperature and therefore of little use in native biologic membranes with vast structural inhomogeneities, the generality becomes apparent when the result is seen as a function of the thermodynamic state of the system and not that of the structure (Schneider, 2011). Furthermore native biological membranes self-organize and even adapt to stay near a criticality in the state diagram of the biological membrane (Hazel, 1995; Hazel et al., 1998; Melchior and Steim, 1976). Laurdan has in fact been used in several of these studies showing that cell membranes change the lipid composition as they adapt to different environmental condition in order to stay in a relatively similar state of fluidity near a transition (Sasaki et al., 2006). Hence the contribution of the mechanism suggested here is expected to be significant in native biological membranes as well, when seen as a function of state and not lipid composition as underlined in Figure.2.

Conclusion

Perturbations in the emission spectrum of solvato-chromic dye Laurdan allowed us to demonstrate that the solvation state of a molecule in the membrane can be modulated acoustically, possibly explaining “sonoporation”. Perturbations due to finite amplitude pressure impulses in the emission spectrum of the membrane probe Laurdan embedded in lipid membranes, have been explained on the basis of fluctuation dissipation theorem. The discussion here does not include cavitation inducing pressure amplitudes, which will be presented as a separate study elsewhere. For such finite amplitude pressure impulses, the width of the emission spectrum quantitatively predicts the specific heat of its environment and hence predicts the membrane response to perturbations or pressure impulses. The local nature of the measurements makes this an immensely powerful experimental technique, as theoretically, it should now be possible to spatially map the heat capacity and other thermodynamic response functions of cellular microenvironments from steady state fluorescence measurements (Sezgin et al., 2015). The ability to do this will help in determining the susceptibility of different cell types or a certain micro environment of theirs to pressure impulses (in general any thermodynamic field) which in turn can help for e.g. find better targets for acoustically triggered therapies.

	System	Agent for state change	Properties measured	Observation	Reference
1	Laurdan in lipid vesicles	Temperature, pH and lipid composition	Emission spectrum and GP (T)	(1) FWHM(T) _{max} in DPPC vesicles at 41C, coincides with PT of DPPC and [d(GP)/dT] _{max} . (2) [d(GP)/dT] _{max} indicates phase transition in vesicles of different lipid composition and different pH	(Parasassi et al., 1991)
2	Laurdan in DMPG vesicles in low ionic strength	Temperature	Emission spectrum and GP (T)	(1) DPMG at low ionic strength has a broad PT starting at 17C and peaking at 35C. (2) FWHM(T) _{max} around 35C which is in the PT region and near [d(GP)/dT] _{max} .	(Lúcio et al., 2010)
3	Laurdan in DPPC vesicles and Tamoxifen	Temperature, Tamoxifen concentration	Emission spectrum, GP(T), heat capacity C, Permeability	(1) Tamoxifen shifts DPPC PT and C _{max} from 41C to lower temperatures. (2) Shift in C _{max} due to tamoxifen coincides with shift in [d(GP)/dT] _{max} to 40C which is further consistent with increase in FWHM. (3) No effect of tamoxifen on FWHM at 35 and 50C as expected from [d(GP)/dT]~0 (4) Temperature and tamoxifen concentration corresponding to FWHM also results in maximum membrane permeability.	(Engelk et al., 2001)
4	Laurdan and Prodan in DSPC vesicles	Pressure and Temperature	Emission Spectrum	(1) FWHM for both Laurdan and Prodan, as a function of pressure, has a maximum at the pressure induced order disorder transition at 63C. (2) Only the FWHM of Prodan has a maximum at pressure induced interdigitated crystalline state at 49C while Laurdan is insensitive.	(Kusube et al., 2005)
5	Prodan in DPPC	Cholesterol and Ethanol	Emission Spectrum	(1) FWHM as a function of cholesterol concentration has a maximum at 15% and 50C. Independently this coincides with the corresponding order-disorder transition in the DPPC/cholesterol phase diagram(82)	(Bondar and Rowe, 1999)
6	Laurdan in POPC and DPPC	Temperature and @-Tocopherol	Emission Spectrum	@-Tocopherol influences FWHM in POPC at 25C as [d(GP)/dT]#0 but not in DPPC as [d(GP)/dT]~0 at 25C	(Massey, 2001)
7	Laurdan in pig kidney basolateral membrane	Cholesterol	GP as a function of cholesterol concentration	Maximum N ⁺ /K ⁺ -ATPase activity coincides with cholesterol concentration corresponding to (d(GP)/d[cholesterol]) _{max}	(69)
8	Laurdan in lipid extracts from human skin stratum corneum (HSC) and bovine brain (BB)	Temperature, pH, lipid composition	GP (T), C(T)	C(T) _{max} coincides with [d(GP)/dT] _{max} for HSC extracts but not for BB extracts, again indicating that Laurdan might not be suitably located to detect all transitions.	(Plasencia et al., 2007)
9	Laurdan in plasma membrane from rat brain cortex	Concentration of Brij58, Triton and Digitonin	Emission Spectra and G-protein activity	(1) Brij 58 and Triton induce a state of increased FWHM while Digitonin does not. (2) Brij58 and Triton concentrations corresponding to FWHM _{max} induce maximum increase in G protein activity while Digitonin does not.	(Sýkora et al., 2009)
10	Laurdan in HIV virus	Methyl-β-cyclodextrin and temperature	Emission spectrum	FWHM _{max} coincides with [d(GP)/dT] _{max}	(Lorizate et al., 2009)

11	Laurdan in brain phosphatidyl serine	Calcium concentration	Excitation and emission spectrum	Narrowing of the spectrum coincides with a blue shift on addition of calcium	(Ramani and Balasubramanian, 2003)
12	Laurdan in Escherichia Coli	Temperature and Chloramphenicol (cam)	Emission Spectra, steady state and time resolved	Peak in [d(GP)/dT] near physiological temperature which shifts to lower temperature on cam treatment. Narrowing of the emission spectra on cooling.	(Vanounou et al., 2002)
13	Laurdan in Rat liver microzomes	Temperature and fatty acids	Emission Spectra and GP	Significant narrowing and blue shift in spectra as a function of temperature	(Garda et al., 1997)

Table 1. Summarizing the experimental studies supporting the derived relationship between fluorescence spectra of an embedded dye and membrane susceptibility. GP represents generalized polarization, C represents heat capacity of the entire sample. GP(T) or C(T) for e.g. implies measured as a function of temperature.

References

- Asano, T., and Okada, T. (1984). "Isomerization of Azobenzenes The Pressure, Solvent, and Substituent Effects," *J. Org. Chem.*, **49**, 4387–4391. doi:10.1021/jo00197a011
- Bagatolli, L. (2003). "Direct observation of lipid domains in free standing bilayers: from simple to complex lipid mixtures," *Chem. Phys. Lipids*, **122**, 137–145. doi:10.1016/S0009-3084(02)00184-6
- Bondar, O. P., and Rowe, E. S. (1999). "Preferential interactions of fluorescent probe Prodan with cholesterol," *Biophys. J.*, **76**, 956–62. doi:10.1016/S0006-3495(99)77259-0
- Bublitz, G., and Boxer, S. (1997). "Stark spectroscopy: applications in chemistry, biology, and materials science," *Annu. Rev. Phys. Chem.*, **48**, 213–242. doi:10.1146/annurev.physchem.48.1.213
- Chowdhury, S., and Chanda, B. (2012). "Perspectives on: conformational coupling in ion channels: thermodynamics of electromechanical coupling in voltage-gated ion channels," *J. Gen. Physiol.*, **140**, 613–23. doi:10.1085/jgp.201210840
- Clarke, R. J., and Kane, D. J. (1997). "Optical detection of membrane dipole potential: avoidance of fluidity and dye-induced effects," *Biochim. Biophys. Acta*, **1323**, 223–39. Retrieved from <http://www.ncbi.nlm.nih.gov/pubmed/9042345>
- Cooper, A. (n.d.). *The Enzyme Catalysis Process*,.
- Diamond, J. M., and Katz, Y. (1974). "Interpretation of nonelectrolyte partition coefficients between dimyristoyl lecithin and water," *J. Membr. Biol.*, **17**, 121–154. doi:10.1007/BF01870176
- Einstein, A. (1901). "Conclusions Drawn from the phenomena of Capilarity," *Ann. Phys.*, **4**, 513–523.
- Einstein, A. (1909). "On the Present Status of the Problem of Radiation," *Ann. Phys.*, **10**, 183–

- Einstein, A. (1910). "Theory of the Opalescence of homogenous fluids and liquid mixtures near the critical state," *Ann. Phys.*, **33**, 1275–1295.
- Einstein, A. (1911). "Discussion following lecture version of 'The present state of the problem of specific heat,'" *Collect. Pap. Albert Einstein*, Princeton University Press, p. 427.
- Einstein, A. (1919). "My theory," *Time*.
- Engelk, M., Bojarski, P., Bloss, R., and Diehl, H. (2001). "Tamoxifen perturbs lipid bilayer order and permeability: comparison of DSC, fluorescence anisotropy, laurdan generalized polarization and carboxyfluorescein leakage studies," *Biophys. Chem.*, **90**, 157–73. Retrieved from <http://www.ncbi.nlm.nih.gov/pubmed/11352274>
- Fenimore, P. W., Frauenfelder, H., McMahon, B. H., and Young, R. D. (2004). "Bulk-solvent and hydration-shell fluctuations, similar to alpha and beta fluctuations in glasses, control protein motions and functions," *Proc. Natl. Acad. Sci.*, **101**, 14408–14413.
- Frauenfelder, H., Alberding, N. a, Ansari, A., Braunstein, D., Cowen, B. R., Hong, M. K., Iben, I. E. T., et al. (1990). "Proteins and Pressure," *J. Phys. Chemistry*, **94**, 1024–1037.
- Frauenfelder, H., Chen, G., Berendzen, J., Fenimore, P. W., Jansson, H., McMahon, B. H., Stroe, I. R., et al. (2009). "A unified model of protein dynamics," *Proc. Natl. Acad. Sci. U. S. A.*, **106**, 5129–34. doi:10.1073/pnas.0900336106
- Garda, H. a, Bernasconi, a M., Brenner, R. R., Aguilar, F., Soto, M. a, and Sotomayor, C. P. (1997). "Effect of polyunsaturated fatty acid deficiency on dipole relaxation in the membrane interface of rat liver microsomes," *Biochim. Biophys. Acta*, **1323**, 97–104. Retrieved from <http://www.ncbi.nlm.nih.gov/pubmed/9030216>
- Grabitz, P., Ivanova, V. P., and Heimburg, T. (2002). "Relaxation kinetics of lipid membranes and its relation to the heat capacity," *Biophys. J.*, **82**, 299–309. doi:10.1016/S0006-3495(02)75395-2
- Halstenberg, S., Heimburg, T., Hianik, T., Kaatze, U., and Krivanek, R. (1998). "Cholesterol-induced variations in the volume and enthalpy fluctuations of lipid bilayers," *Biophys. J.*, **75**, 264–71. doi:10.1016/S0006-3495(98)77513-7
- Harris, F. (2002). "Use of laurdan fluorescence intensity and polarization to distinguish between changes in membrane fluidity and phospholipid order," *Biochim. Biophys. Acta - Biomembr.*, **1565**, 123–128. doi:10.1016/S0005-2736(02)00514-X
- Harris, F. M., Best, K. B., and Bell, J. D. (2002). "Use of laurdan fluorescence intensity and polarization to distinguish between changes in membrane fluidity and phospholipid order," *Biochim. Biophys. Acta*, **1565**, 123–8. Retrieved from <http://www.ncbi.nlm.nih.gov/pubmed/12225860>
- Hazel, J. (1995). "Thermal adaptation in biological membranes: is homeoviscous adaptation the explanation?," *Annu. Rev. Physiol.*, Retrieved from <http://www.annualreviews.org/doi/pdf/10.1146/annurev.ph.57.030195.000315>. Retrieved from <http://www.annualreviews.org/doi/pdf/10.1146/annurev.ph.57.030195.000315>
- Hazel, J. R., McKinley, S. J., and Gerrits, M. F. (1998). "Thermal acclimation of phase behavior in plasma membrane lipids of rainbow trout hepatocytes," *Am. J. Physiol.*, **275**, R861-9.

Retrieved from <http://www.ncbi.nlm.nih.gov/pubmed/9728085>

- Heimburg, T. (1998). "Mechanical aspects of membrane thermodynamics Estimation of the mechanical properties of lipid membranes close to the chain melting transition from calorimetry," *Biochim. Biophys. Acta - Biomembr.*, **1415**, 147–162. doi:10.1016/S0005-2736(98)00189-8
- Honerkamp-Smith, A. R., Cicuta, P., Collins, M. D., Veatch, S. L., den Nijs, M., Schick, M., and Keller, S. L. (2008). "Line tensions, correlation lengths, and critical exponents in lipid membranes near critical points," *Biophys. J.*, **95**, 236–46. doi:10.1529/biophysj.107.128421
- Jaffe, H., and Miller, A. (1966). "The fates of electronic excitation energy," *J. Chem. Educ.*, **43**, 469–473.
- Kadhim, A. H. (1966). "High Pressures on the Absorption Spectrum of Azobenzene'," **973**, 1805–1809.
- Kaufmann, K. (1989). *On the role of phospholipid membrane in free energy coupling*, Caruaru, Brasil, 1st ed. Retrieved from <https://sites.google.com/site/schneiderslab/research-group/literature>
- Kessler, L. W., and Dunn, F. (1969). "Ultrasonic investigation of the conformational changes of bovine serum albumin in aqueous solution," *J. Phys. Chem.*, **73**, 4256–63. doi:10.1021/j100846a037
- Koshiyama, K., Kodama, T., Yano, T., and Fujikawa, S. (2006). "Structural Change in Lipid Bilayers and Water Penetration Induced by Shock Waves: Molecular Dynamics Simulations," *Biophys. J.*, **91**, 2198–2205. doi:10.1529/biophysj.105.077677
- Krasovitski, B., Frenkel, V., Shoham, S., and Kimmel, E. (2011). "Intramembrane cavitation as a unifying mechanism for ultrasound-induced bioeffects," *Proc. Natl. Acad. Sci. U. S. A.*, **108**, 3258–63. doi:10.1073/pnas.1015771108
- Krivanek, R., Okoro, L., and Winter, R. (2008). "Effect of cholesterol and ergosterol on the compressibility and volume fluctuations of phospholipid-sterol bilayers in the critical point region: a molecular acoustic and calorimetric study," *Biophys. J.*, **94**, 3538–48. doi:10.1529/biophysj.107.122549
- Kudo, N., Okada, K., and Yamamoto, K. (2009). "Sonoporation by single-shot pulsed ultrasound with microbubbles adjacent to cells," *Biophys. J.*, **96**, 4866–76. doi:10.1016/j.bpj.2009.02.072
- Kusube, M., Tamai, N., Matsuki, H., and Kaneshina, S. (2005). "Pressure-induced phase transitions of lipid bilayers observed by fluorescent probes Prodan and Laurdan," *Biophys. Chem.*, **117**, 199–206. doi:10.1016/j.bpc.2005.05.007
- Legon, W., Sato, T. F., Opitz, A., Mueller, J., Barbour, A., Williams, A., and Tyler, W. J. (2014). "Transcranial focused ultrasound modulates the activity of primary somatosensory cortex in humans," *Nat. Neurosci.*, **17**, 322–9. doi:10.1038/nn.3620
- Lorzate, M., Brügger, B., Akiyama, H., Glass, B., Müller, B., Anderluh, G., Wieland, F. T., et al. (2009). "Probing HIV-1 membrane liquid order by Laurdan staining reveals producer cell-dependent differences," *J. Biol. Chem.*, **284**, 22238–47. doi:10.1074/jbc.M109.029256
- Lúcio, A. D., Vequi-Suplicy, C. C., Fernandez, R. M., and Lamy, M. T. (2010). "Laurdan

- spectrum decomposition as a tool for the analysis of surface bilayer structure and polarity: a study with DMPG, peptides and cholesterol," *J. Fluoresc.*, **20**, 473–82. doi:10.1007/s10895-009-0569-5
- Luzzati, V., Mateu, L., Marquez, G., and Borgo, M. (1999). "Structural and electrophysiological effects of local anesthetics and of low temperature on myelinated nerves: implication of the lipid chains in nerve excitability," *J. Mol. Biol.*, **286**, 1389–402. doi:10.1006/jmbi.1998.2587
- Marcus, R. A., and Amos, A. (1985). "Electron transfers in chemistry and biology and Norman Sutin b," **811**, 265–322.
- Massey, J. B. (2001). "Interfacial properties of phosphatidylcholine bilayers containing vitamin E derivatives," *Chem. Phys. Lipids*, **109**, 157–74. Retrieved from <http://www.ncbi.nlm.nih.gov/pubmed/11269935>
- Mauring, K., Deich, J., Rosell, F. I., McAnaney, T. B., Moerner, W. E., and Boxer, S. G. (2005). "Enhancement of the fluorescence of the blue fluorescent proteins by high pressure or low temperature," *J. Phys. Chem. B*, **109**, 12976–81. doi:10.1021/jp0448595
- Melchior, D., and Steim, J. (1976). "Thermotropic transitions in biomembranes," *Annu. Rev. Biophys. Bioeng.*, **5**, 205–238. Retrieved from <http://www.annualreviews.org/doi/abs/10.1146/annurev.bb.05.060176.001225>
- Munro, S. (2003). "Lipid Rafts : Elusive or Illusive ? Review," *Cell*, **115**, 377–388.
- Needham, D., and Evans, E. (1988). "Structure and mechanical properties of giant lipid (DMPC) vesicle bilayers from 20 degrees C below to 10 degrees C above the liquid crystal-crystalline phase transition at 24 degrees C," *Biochemistry*, **27**, 8261–9. Retrieved from <http://www.ncbi.nlm.nih.gov/pubmed/3233209>
- O'Brien, W. D., and Dunn, F. (1972). "Ultrasonic absorption in aqueous solutions of Bovine Hemoglobin," *J. Phys. Chem.*, **76**, 528–533. doi:10.1021/j100717a017
- Owen, D. M., and Gaus, K. (2009). "Optimized time-gated generalized polarization imaging of Laurdan and di-4-ANEPPDHQ for membrane order image contrast enhancement," *Microsc. Res. Tech.*, **9999**, NA-NA. doi:10.1002/jemt.20801
- Owen, D. M., Lanigan, P. M. P., Dunsby, C., Munro, I., Grant, D., Neil, M. A. A., French, P. M. W., et al. (2006). "Fluorescence lifetime imaging provides enhanced contrast when imaging the phase-sensitive dye di-4-ANEPPDHQ in model membranes and live cells," *Biophys. J.*, **90**, L80-2. doi:10.1529/biophysj.106.084673
- Papahadjopoulos, D., and Moscarello, M. (1975). "Effects of proteins on the thermotropic phase transitions of phospholipid membranes," *Biochim. Biophys. ...*, **401**, 317–335. Retrieved from <http://www.sciencedirect.com/science/article/pii/0005273675902333>
- Parasassi, T., Krasnowska, E. K., Bagatolli, L., and Gratton, E. (1998). "Laurdan and Prodan as Polarity-Sensitive Fluorescent Membrane Probes," **8**, 365–373.
- Parasassi, T., Ravagnan, G., Rusch, R. M., and Gratton, E. (1993). "Modulation and dynamics of phase properties in phospholipid mixtures detected by Laurdan fluorescence," *Photochem. Photobiol.*, **57**, 403–410. doi:10.1111/j.1751-1097.1993.tb02309.x
- Parasassi, T., De Stasio, G., d'Ubaldo, a, and Gratton, E. (1990). "Phase fluctuation in

- phospholipid membranes revealed by Laurdan fluorescence,” *Biophys. J.*, **57**, 1179–86. doi:10.1016/S0006-3495(90)82637-0
- Parasassi, T., Stasio, G. De, Ravagnan, G., Rusch, R. M., and Gratton, E. (1991). “Quantitation of lipid phases in phospholipid vesicles by the generalized polarization of laurdan fluorescence,” *Biophys. J.*, **60**, 179–189.
- Plasencia, I., Norlén, L., and Bagatolli, L. a (2007). “Direct visualization of lipid domains in human skin stratum corneum’s lipid membranes: effect of pH and temperature,” *Biophys. J.*, **93**, 3142–55. doi:10.1529/biophysj.106.096164
- Poperscu, A., Radu, M., Zorilla, B., and Bacalum, M. (2013). “Laurdan solvatochromism : Influence of solvent polarity and hydrogen bonds,” *Optoelectron. Adv. Mater. - rapid Commun.*, **7**, 456–460.
- Prakash, M. K., and Marcus, R. a (2007). “An interpretation of fluctuations in enzyme catalysis rate, spectral diffusion, and radiative component of lifetimes in terms of electric field fluctuations,” *Proc. Natl. Acad. Sci. U. S. A.*, **104**, 15982–7. doi:10.1073/pnas.0707859104
- Ramani, K., and Balasubramanian, S. V (2003). “Fluorescence properties of Laurdan in cochleate phases,” *Biochim. Biophys. Acta - Biomembr.*, **1618**, 67–78. doi:10.1016/j.bbamem.2003.10.009
- Rigler, R. (2010). “Fluorescence and single molecule analysis in cell biology,” *Biochem. Biophys. Res. Commun.*, **396**, 170–5. doi:10.1016/j.bbrc.2010.04.070
- Sanchez, S. a, Tricerri, M. a, and Gratton, E. (2012). “Laurdan generalized polarization fluctuations measures membrane packing micro-heterogeneity in vivo,” *Proc. Natl. Acad. Sci. U. S. A.*, **109**, 7314–9. doi:10.1073/pnas.1118288109
- Sasaki, T., Konoha, Y., Toyoda, T., Yasaka, Y., Przybos, E., and Nakaoka, Y. (2006). “Correlation between thermotolerance and membrane properties in *Paramecium aurelia*,” *J. Exp. Biol.*, **209**, 3580–6. doi:10.1242/jeb.02426
- Schneider, M. (2011). *Thermodynamic States and Transitions as the Foundation of Biological Functions: Self-Organized Blood and Einstein ’ s view on Soft Interfaces* Havblitation, University of Augsburg, 4 pages.
- Seeger, H. M., Aldrovandi, L., Alessandrini, A., and Facci, P. (2010). “Changes in single K(+) channel behavior induced by a lipid phase transition,” *Biophys. J.*, **99**, 3675–83. doi:10.1016/j.bpj.2010.10.042
- Sezgin, E., Waithe, D., Bernardino De La Serna, J., and Eggeling, C. (2015). “Spectral imaging to measure heterogeneity in membrane lipid packing,” *ChemPhysChem*, **16**, 1387–1394. doi:10.1002/cphc.201402794
- Shimomura, M., and Kunitake, T. (1987). “Fluorescence and Photoisomerization of Azobenzene-Containing Bilayer Membranes,” **33**, 5175–5183.
- Shrivastava, S., and Schneider, M. F. (2013). “Opto-Mechanical Coupling in Interfaces under Static and Propagative Conditions and Its Biological Implications,” *PLoS One*, **8**, 2005–2007. doi:10.1371/journal.pone.0067524
- Shrivastava, S., and Schneider, M. F. (2014). “Evidence for two-dimensional Solitary Sound Waves in a Lipid Controlled Interface and its Biological Implications for Biological

- Signaling,” *J. R. Soc. Interface*, **11**, 1–8. doi:10.1098/rsif.2014.0098
- Sotomayor, C. P., Aguilar, L. F., Cuevas, F. J., Helms, M. K., and Jameson, D. M. (2000). “Modulation of pig kidney Na⁺/K⁺-ATPase activity by cholesterol: role of hydration,” *Biochemistry*, **39**, 10928–35. Retrieved from <http://www.ncbi.nlm.nih.gov/pubmed/10978181>
- Steppich, D., Griesbauer, J., Frommelt, T., Appelt, W., Wixforth, a., and Schneider, M. (2010). “Thermomechanic-electrical coupling in phospholipid monolayers near the critical point,” *Phys. Rev. E*, **81**, 1–5. doi:10.1103/PhysRevE.81.061123
- Sýkora, J., Bourová, L., Hof, M., and Svoboda, P. (2009). “The effect of detergents on trimeric G-protein activity in isolated plasma membranes from rat brain cortex: correlation with studies of DPH and Laurdan fluorescence,” *Biochim. Biophys. Acta*, **1788**, 324–32. doi:10.1016/j.bbamem.2008.11.008
- Szilágyi, A., Selstam, E., and Akerlund, H.-E. (2008). “Laurdan fluorescence spectroscopy in the thylakoid bilayer: the effect of violaxanthin to zeaxanthin conversion on the galactolipid dominated lipid environment,” *Biochim. Biophys. Acta*, **1778**, 348–55. doi:10.1016/j.bbamem.2007.10.006
- Tasaki, I., Carbone, E., Sisco, K., and Singer, I. (1973). “Spectral analyses of extrinsic fluorescence of the nerve membrane labeled with aminonaphthalene derivatives,” *Biochim. Biophys. Acta (BBA ...)*, **323**, 220–233. Retrieved from <http://www.sciencedirect.com/science/article/pii/0005273673901466>
- Tatat, D. B., and Dunn, F. (1992). “Ultrasound and Model Membrane Systems: Analyses and Predlctions,” *J. Phys. Chem.,.*
- Titova, T. Y., Artyukhov, V. Y., Zharkova, O. M., and Morozova, J. P. (2014). “Spectral-luminescent properties of lauridan molecule,” *Spectrochim. Acta - Part A Mol. Biomol. Spectrosc.,* **124**, 64–69. doi:10.1016/j.saa.2013.12.097
- Toyoda, T., Hiramatsu, Y., Sasaki, T., and Nakaoka, Y. (2009). “Thermo-sensitive response based on the membrane fluidity adaptation in *Paramecium multimicronucleatum*,” *J. Exp. Biol.,* **212**, 2767–72. doi:10.1242/jeb.031278
- Ulrich, A. S., Sami, M., and Watts, A. (1994). “Hydration of DOPC bilayers by differential scanning calorimetry,” *BBA - Biomembr.,* **1191**, 225–230. doi:10.1016/0005-2736(94)90253-4
- Vanounou, S., Pines, D., Pines, E., Parola, A. H., and Fishov, I. (2002). “Coexistence of domains with distinct order and polarity in fluid bacterial membranes,” *Photochem. Photobiol.,* **76**, 1–11. Retrieved from <http://www.ncbi.nlm.nih.gov/pubmed/12126299>
- De Vequi-Suplicy, C. C., Benatti, C. R., and Lamy, M. T. (2006). “Laurdan in fluid bilayers: position and structural sensitivity,” *J. Fluoresc.,* **16**, 431–9. doi:10.1007/s10895-005-0059-3
- Viard, M., Gallay, J., Vincent, M., Meyer, O., Robert, B., and Paternostre, M. (1997). “Laurdan solvatochromism: solvent dielectric relaxation and intramolecular excited-state reaction,” *Biophys. J.,* **73**, 2221–34. doi:10.1016/S0006-3495(97)78253-5
- Viard, M., Gallay, J., Vincent, M., and Paternostre, M. (2001). “Origin of lauridan sensitivity to the vesicle-to-micelle transition of phospholipid-octylglucoside system: a time-resolved fluorescence study,” *Biophys. J.,* **80**, 347–59. doi:10.1016/S0006-3495(01)76019-5

- Wang, Y., Jing, G., Perry, S., Bartoli, F., and Tatic-Lucic, S. (2009). "Spectral characterization of the voltage-sensitive dye di-4-ANEPPDHQ applied to probing live primary and immortalized neurons," *Opt. Express*, **17**, 984–90. Retrieved from <http://www.ncbi.nlm.nih.gov/pubmed/19158915>
- Wazawa, T., Ishii, Y., Funatsu, T., Yanagida, T., Baldwin, T. O., Christophore, J. A., Raushel, F. M., et al. (2000). "Spectral fluctuation of a single fluorophore conjugated to a protein molecule," *Biophys. J.*, **78**, 1561–9. doi:10.1016/S0006-3495(00)76708-7
- Wilkinson, D. A., and Nagle, J. F. (1982). "Specific heats of lipid dispersions in single phase regions," *Biochim. Biophys. Acta - Biomembr.*, **688**, 107–115. doi:10.1016/0005-2736(82)90584-3
- Wunderlich, B., Leirer, C., Idzko, A., Keyser, U. F., Wixforth, A., Myles, V. M., and Heimburg, T. (2009). "Phase-State Dependent Current Fluctuations in Pure Lipid Membranes," *Biophysj*, **96**, 4592–4597. doi:10.1016/j.bpj.2009.02.053
- Xin Chen, Tinglu Yang, Sho Kataoka, and, and Cremer*, P. S. (2007). "Specific Ion Effects on Interfacial Water Structure near Macromolecules," , doi: 10.1021/JA073869R. doi:10.1021/JA073869R
- Zheng, J., Chin, W.-C., Khijniak, E., Khijniak, E., and Pollack, G. H. (2006). "Surfaces and interfacial water: Evidence that hydrophilic surfaces have long-range impact," *Adv. Colloid Interface Sci.*, **127**, 19–27. doi:10.1016/j.cis.2006.07.002
- Zhou, Y., Kumon, R. E., Cui, J., and Deng, C. X. (2009). "The size of sonoporation pores on the cell membrane," *Ultrasound Med. Biol.*, **35**, 1756–60. doi:10.1016/j.ultrasmedbio.2009.05.012
- Zhu, Y., and Granick, S. (2001). "Viscosity of Interfacial Water," *Phys. Rev. Lett.*, **87**, 96104. doi:10.1103/PhysRevLett.87.096104